

# Spin noise spectroscopy of rubidium atomic gas under resonant and non-resonant conditions\*

Jian Ma(马健)<sup>1</sup>, Ping Shi(史平)<sup>1</sup>, Xuan Qian(钱轩)<sup>1</sup>, Wei Li(李伟)<sup>2</sup>, and Yang Ji(姬扬)<sup>1,†</sup>

<sup>1</sup>SKLSM, Institute of Semiconductors, Chinese Academy of Science, Beijing 100083, China      <sup>2</sup>Faculty of Maritime Technology and Operations, Norwegian University of Science and Technology, Aalesund 6025, Norway

(Received 7 July 2016; revised manuscript received 11 August 2016; published online 28 September 2016)

The spin fluctuation in rubidium atom gas is studied via all-optical spin noise spectroscopy (SNS). Experimental results show that the integrated SNS signal and its full width at half maximum (FWHM) strongly depend on the frequency detuning of the probe light under resonant and non-resonant conditions. The total integrated SNS signal can be well fitted with a single squared Faraday rotation spectrum and the FWHM dependence may be related to the absorption profile of the sample.

**Keywords:** spin noise spectroscopy, rubidium atoms, homogeneous broaden

**PACS:** 72.25.Rb, 42.50.Lc, 32.30.-r, 42.25.Bs

**DOI:** 10.1088/1674-1056/25/11/117203

## 1. Introduction

Most experimental studies of spin dynamics rely on the generation of a non-equilibrium spin polarization.<sup>[1]</sup> Extra energy has to be pumped into the system to create a spin polarization, thus leading to additional mechanisms of spin dephasing. Such a problem may be avoided in an all-optical spin noise spectroscopy (SNS), which perturbs the system minimally. The SNS technique uses a linearly polarized, below-band-gap laser as the probe light to sense the Faraday rotation (FR) of the system. The FR results from the projection of average spin polarization on the direction of light propagation, which fluctuates even in the thermal equilibrium condition.<sup>[2]</sup>

SNS measurements were first carried out in atom optics by Crooker *et al.*, who measured the spin fluctuations in Rb and K atom vapors.<sup>[3]</sup> Oestreich and co-workers applied this technique to semiconductors and measured the spin lifetime of electrons in n-GaAs at low temperature.<sup>[4]</sup> To improve the measurement efficiency and precision, Crooker *et al.* used digitizers incorporating on-board field programmable gate array (FPGA) processors to perform fast Fourier transform in real time with a sampling rate up to 1 GHz.<sup>[5]</sup> This hardware method enabled a much higher signal to noise ratio, leading to more works on spin-related physics in low-dimensional semiconductors during the past few years. In 2012, SNS studies were reported on quantum dot ensembles whose signal comes from about 50 holes.<sup>[6,7]</sup> Oestreich *et al.* pushed the SNS technique down to the single spin detection regime and studied the spin relaxation dynamic of a single heavy hole localized in a single (InGa)As quantum dot in 2014.<sup>[8]</sup> In 2015, SNS was used to study nuclear spin dynamics in n-type GaAs.<sup>[9,10]</sup>

Another interesting experiment was performed by Roy *et al.*, who used “two-color” optical spin noise spectroscopy to explore spin interactions between different spin ensembles.<sup>[11]</sup> In addition, Li *et al.* developed theoretical methods to explore higher-order (third and fourth) cumulants of the spin noise in the frequency domain.<sup>[12,13]</sup>

A lot of works have been done both theoretically and experimentally to understand the spin noise. Oestreich *et al.* did SNS measurements under resonant as well as non-resonant probing conditions in an inhomogeneously broadened optical system (Rb vapor with 1 mbar of He buffer gas), and found that the SNS signal amplitude depends not only on the coherence between the ground and the excited states, but also on the ground-ground and excited-excited coherences in resonant and quasi-resonant probing conditions.<sup>[14]</sup> Crooker and co-workers studied the spin fluctuations of resident holes in (In,Ga)As quantum dots and 4S electrons in <sup>41</sup>K atoms respectively, showing that the SNS at different frequency depends on homogeneously and inhomogeneously broadened optical bands of the samples.<sup>[15]</sup>

The above studies focused on the line shape of the SNS signal at different frequencies, which can reveal some information of the sample. Here, we put emphasis on the difference of the SNS signal and the spin dephasing time measured between resonant and non-resonant conditions. We use a self-made SNS system to study the spin fluctuations at different frequencies in natural rubidium gas. The sample also contains nitrogen buffer gas of 250 torr and it is a homogeneously broadened optical system. The SNS amplitude and its full width at half maximum (FWHM) are measured and analyzed.

\*Project supported by the National Natural Science Foundation of China (Grant Nos. 91321310 and 11404325) and the National Basic Research Program of China (Grant No. 2013CB922304).

†Corresponding author. E-mail: jiyang@semi.ac.cn

## 2. Experimental setup

The basic idea of SNS is to map the stochastic fluctuation in the sample onto the polarization of the laser light. Its principle is shown in Fig. 1. A linearly polarized laser light is transmitted through the sample, which is Rb atom gas in our case. The atom ensemble shows stochastic spin polarization at a given time. This results in different absorption of right ( $\sigma^-$ ) and left ( $\sigma^+$ ) circularly polarized light, which leads to a difference of the dispersive part of the refractive indices for the two circular light components (the Kramers–Kronig relation).

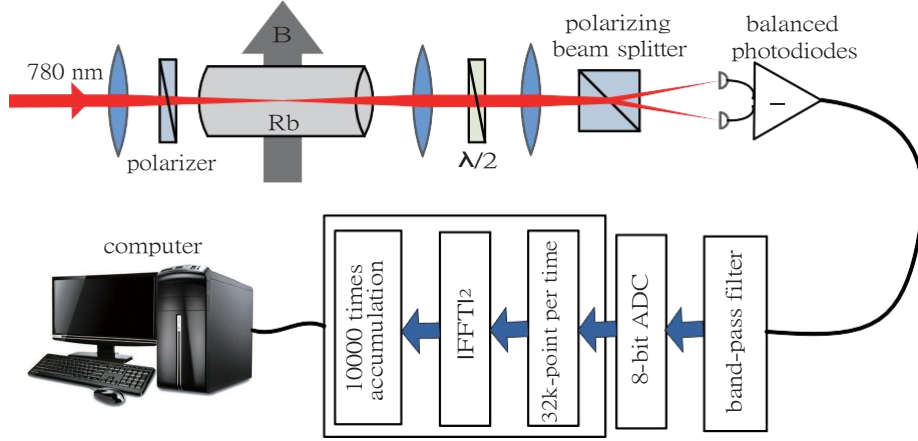


**Fig. 1.** (color online) Schematic of experimental setup for rubidium spin noise spectrum measurement. Random fluctuation of the FR signal is detected by a balanced photodiode bridge and an FPGA-based DAC.

The light beam comes from a linearly polarized Ti:sapphire continue-wave tunable laser with a spectral line width of about 100 kHz. It is focused by a lens with 400 mm focal length to a beam diameter of 100  $\mu\text{m}$  at the center of the Rb vapor cell. The laser is swept with a tuning range of  $-18$  GHz to 18 GHz relative to the D2 transition ( $5^2S_{1/2}$  to  $5^2P_{3/2}$ ) of Rb around 780 nm.

The FR signal is collected and analyzed via an FPGA-based DAC with a sampling rate up to 1 GHz. The input range of the DAC is from  $-0.5$  V to  $+0.5$  V, with an 8-bit resolution. An electrical band-pass filter with 0.5 MHz low cut-off frequency is used before the high-speed DAC. An FPGA processor does fast-Fourier transform (FFT) per 32k-points in real time, while the DAC reads data continuously.<sup>[16]</sup> 10000 power spectra are accumulated before the results are sent to a computer. While a traditional spectrum analyzer has a data utilization ratio of about 0.1%,<sup>[5]</sup> our DAC board is about 50%, which could be further improved by increasing the data transmission speed between the computer and the DAC.

A uniform magnetic field is provided by a Helmholtz coil with its direction perpendicular to the laser propagation. This shifts the spin noise peaks away from zero frequency to the Larmor precession frequency  $\nu_L = g\mu_B B/h$  ( $g$  is the Lande' factor,  $\mu_B$  is the Bohr magneton,  $B$  is the external magnetic field, and  $h$  is the Plank constant). The magnetic field is alternated between zero and a finite value (a few tens of Gauss).

The linearly polarized probe laser light, which is composed of  $\sigma^-$  and  $\sigma^+$  light, acquires a rotation of its linear polarization direction due to the circular birefringence, the Faraday effect. The variation of the Faraday rotation (FR) angle of the probe light is measured via a balanced photodiode bridge, which consists of a balanced photoreceiver and a polarization beam splitter oriented at  $45^\circ$  to the incident laser polarization. The output signal of the balanced photoreceiver is sent to an FPGA-based data acquisition card (DAC) and finally collected by a computer.

Each spectrum is typically averaged for 15 min. In order to remove the photon shot noise and the residual electrical noise, the background spectrum acquired at zero field is subtracted from the spectrum at finite magnetic field. Usually a 10 G magnetic field is applied to avoid the low-frequency noise from the experimental environment and hyperfine splitting of SNS under high external magnetic field. In this work, we use a 60 mm long glass cell which contains natural rubidium vapor with isotopes  $^{85}\text{Rb}$  (72.15%) and  $^{87}\text{Rb}$  (27.85%). The radiation trapping and collision rate with the cell walls are reduced by introducing 250 torr  $\text{N}_2$  buffer gas. A furnace is used to control the temperature of the cell, thus tuning the gas density of the Rb gas.

## 3. Results and discussion

The SNS gives information about the Lande' factor and the transverse spin lifetime. The Lande' factor depends on the total angular momentum quantum number  $F$  and is given by  $g_F = h\nu_L/\mu_B B$ , where  $\nu_L$  is the Larmor frequency corresponding to the position of the SNS peak. Figure 2(b) depicts a typical SNS trace from rubidium vapor. The laser is detuned 7 GHz below the D2 transition ( $5^2S_{1/2}$  to  $5^2P_{3/2}$ ). The spin noise signal peaks at 4.76 MHz and 7.11 MHz corresponding to random spin fluctuations that are precessing in the 10 G transverse magnetic field. Effective  $g$ -factors  $g_F \approx 0.339$  and

0.508 are the ground-state  $g$ -factors of the isotopes  $^{85}\text{Rb}$  and  $^{87}\text{Rb}$ , respectively. They are well agreed with the theoretical values of  $g_F = 1/3$  and  $1/2$ . The spin noise peak position moves linearly with the magnetic field  $B$ , as indicated in the inset of Fig.2(b). The SNS traces can be well fitted by a single Lorentz fit and the FWHM of the Lorentzian line shape  $\Delta\nu$  directly yields the transverse spin lifetime  $T_2 = 1/\Delta\nu$ . The FWHM of the spin noise peaks in Fig.2(b) amounts to 70 kHz, indicating that the transverse spin lifetime is about 14  $\mu\text{s}$ , much shorter than the known Rb spin lifetime (about 100 ms<sup>[17]</sup>) and the transit time of the Rb atoms across the 100  $\mu\text{m}$  laser diameter (0.2 ms). The DAC used in the experiment does FFT per 32k-points with sampling rate 1 GHz, meaning that each trace lasts no more than 32  $\mu\text{s}$ , thus the

resolution of the DAC is 32 kHz. This explains why the transverse spin lifetime measured by SNS is shorter than that by the other methods. The inset of Fig.2(b) shows that the line width of the spin noise peak increases and the amplitude of the signal decreases as the magnetic field  $B$  increases. However, the integrated spin noise is constant to within 8% in different magnetic fields. This is due to the gradual decoupling of the electron and nuclear spins by the applied magnetic field.<sup>[3]</sup> Take  $^{87}\text{Rb}$  for example, in Fig.2(c), we can see that the spin noise peaks breakup into distinct peaks at  $B = 45$  G when the spin coherences between all allowed  $\Delta F = 0$ ,  $\Delta m_F = \pm 1$  Zeeman transitions are resolved. The schematic diagram of the ground-state hyperfine interaction (Fig.2(d)) and the split spin noise peaks can be placed in one-to-one correspondence.

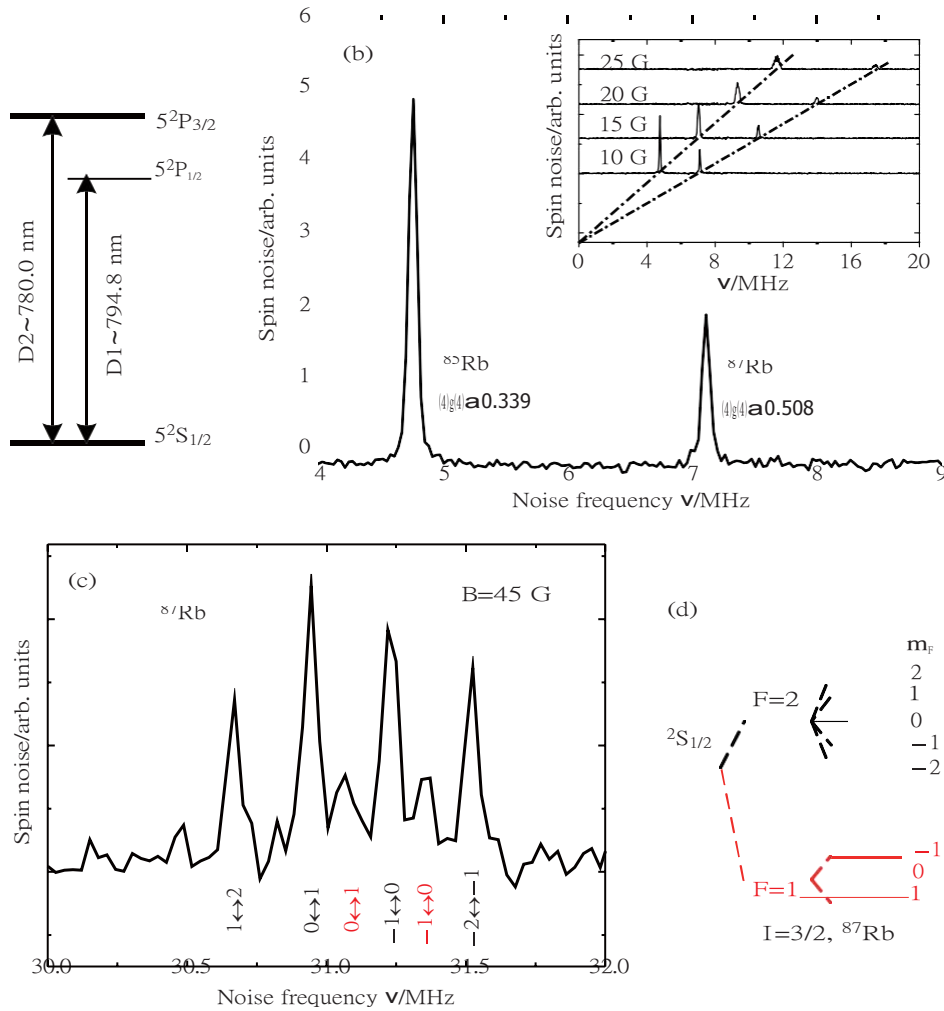


**Fig. 2.** (color online) Spontaneous spin noise in Rb at temperature  $T = 343$  K. The laser is detuned  $\Omega_{D2} = 7$  GHz from the D2 transition ( $5^2S_{1/2}$  to  $5^2P_{3/2}$ , 780 nm), ensuring negligible absorption. The laser power  $P = 300$   $\mu\text{W}$ . (a) D-line transition structure of Rb. (b) SNS in magnetic field  $B = 10$  G. Inset: SNS traces in different magnetic field  $B$ . (c) SNS of  $^{87}\text{Rb}$  in magnetic field  $B = 45$  G. (d) Schematic diagram of the ground-state hyperfine levels of  $^{87}\text{Rb}$ , nuclear spin  $I = 3/2$ .

The SNS signal can be obtained under non-resonant and resonant conditions in atom gas. So far we have given the results of the former case, which denotes the spin dynamics of

Rb under non-resonant condition. Next, we will give the SNS measured under resonant and quasi-resonant conditions which can reveal additional information of the spin system.<sup>[14,15]</sup> We

will focus on the difference of the SNS measured under resonant and non-resonant conditions in the Rb vapor. Figure 3(a) depicts the SNS power density as a function of laser detuning. The integrated SNS is symmetrical relative to the central frequency of the absorption spectrum. Under the quasi-resonant condition, the closer it is to the central frequency, the larger the power intensity of SNS is. However, the power intensity becomes smaller when the laser frequency is closer to the central frequency under the resonant condition. At the central frequency of the absorption spectrum, the signal of SNS approaches zero.

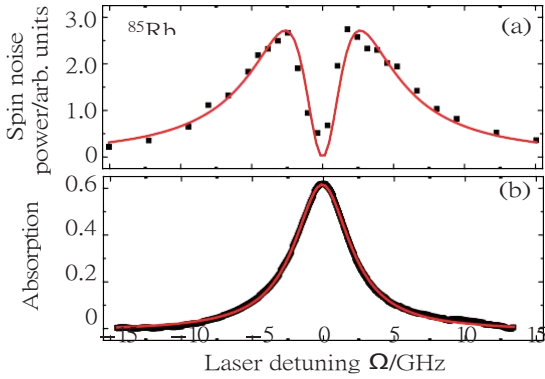


**Fig. 3.** (color online) Ground state spin fluctuation of  $^{85}\text{Rb}$  at different detunings of the probe laser from the D2 optical transition. The laser power  $P = 300 \mu\text{W}$ ,  $T = 318 \text{ K}$ ,  $B = 10 \text{ G}$ . (a) Integrated SNS (black squares) and fitting curve (red lines) as a function of the laser detuning from the D2 transition of  $^{85}\text{Rb}$ . (b) The absorption spectrum of Rb.

To interpret the SNS line shape dependence on the laser frequency, we should first get some information about the optical absorption of the system. Such a property can be revealed in its absorption spectrum, as shown in Fig. 3(b). The FWHM of the absorption spectrum at  $T = 318 \text{ K}$  is about 4.7 GHz, while the calculated Doppler broadening is about 560 MHz, meaning that the line broadening of the absorption spectrum mainly comes from pressure-broadened by 250 torr  $\text{N}_2$  and the system is homogeneously broadened. Thus, the fluctuations of the FR will be evidently correlated over the whole spectrum and all the spins of the system are identical. The FR spectrum of the system can be calculated by

$$\theta(\Omega) = \frac{\Omega_0 - \Omega}{(\Omega_0 - \Omega)^2 + (\gamma/2)^2}, \quad (1)$$

where  $\Omega$  is the laser frequency,  $\Omega_0$  is the resonance frequency, and  $\gamma$  is the homogeneous line width of the absorption spectrum. The FR noise ( $\delta\theta^2(\Omega)$ ) is proportional to the square of the FR

$$(\delta\theta^2(\Omega)) \sim \theta^2(\Omega). \quad (2)$$

Therefore, a single squared FR spectrum can fit well the experiment data.<sup>[15]</sup>

The measured FWHM of the noise peaks indicates the effective transverse spin dephasing time, which is given by  $T_2 = 1/(\Delta\nu)$ . Figure 4 shows the FWHM dependence of SNS on the probe laser frequency in  $^{85}\text{Rb}$ . The FWHM of  $^{85}\text{Rb}$  is almost constant when the optical absorption becomes negligible. It gets broader as the laser frequency moves closer to the center frequency of the absorption. Lorentz fit is used to verify the experiment data and the FWHM of the fitting curve is equal to the FWHM of the absorption spectrum (Fig. 3(b)).

In the following, we give an explanation to the dependency of the FWHM of SNS on the probe laser frequency. The transverse spin dephasing time is calculated by<sup>[18-20]</sup>

$$\frac{1}{T_2} = \frac{1}{T_0} + \frac{1}{T_{\text{absorption}}}, \quad (3)$$

where  $T_0$  is the spin relaxation due to buffer-gas collisions, the transit time of the atoms across the light beam, and the resolution of the DAC.  $T_{\text{absorption}}$  indicates the contribution from absorption of photons from the probe light. The probe light is a linear polarized beam, and a single photon has arbitrary helicity, so the spin polarization of an atom is destroyed by the absorption since the absorption of a probe light photon changes the atom's angular momentum. The absorption spectrum has a Lorentzian line shape in a homogeneously broadened optical system (see Fig. 3(b)). Hence, the FWHM of SNS as a function of the laser frequency can be computed as

$$\Delta\nu = \Delta\nu_0 + A \frac{\gamma}{\gamma^2 + 4(\Omega_0 - \Omega)^2}, \quad (4)$$

where  $A$  is a parameter depending on the gas density.

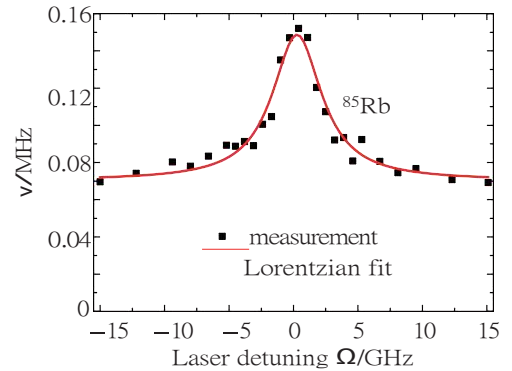


**Fig. 4.** (color online) The FWHM of SNS ( $^{85}\text{Rb}$ ) as a function of laser frequency detuning. The black squares and red line indicate the experimental data and the fitting curve, respectively.

## 4. Conclusion

The spin noise spectroscopy provides a unique opportunity to study the magnetic resonance and spin dynamics of atoms in a perturbation-free way, and some remarkable properties can be obtained by SNS under the resonant condition. We have studied the difference of FR noise at different probe

frequencies near the D2 transition of Rb atoms. The experimental results show that the integrated SNS signal is proportional to the square of FR in the homogeneously broadened optical system. The difference of spin lifetime under different frequencies may come from the light absorption during light propagation in the Rb vapor. This study may help understand the spin noise spectrum and increase its applications.

## Acknowledgment

We thank Professor Yuansen Chen and Professor Mingsheng Zhan for our helpful discussions.

## References

- [1] Müller G M, Oestreich M, Römer M and Hübner J 2010 *Physica E* **43** 569
- [2] Dyakonov M I 2008 *Spin Physics in Semiconductors* (Berlin: Springer-Verlag) p. 129
- [3] Crooker S A, Rickel D G, Balatsky A V and Smith D L 2004 *Nature* **431** 49
- [4] Oestreich M, Römer M, Haug R J and Hägele D 2005 *Phys. Rev. Lett.* **95** 216603
- [5] Crooker S A, Brandt J, Sandfort C, Greilich A, Yakovlev D R, Reuter D, Wieck A D and Bayer M 2010 *Phys. Rev. Lett.* **104** 036601
- [6] Dabhashi R, Hübner J, Berski F, Wiegand J, Marie X, Pierz K, Schumacher H W and Oestreich M 2012 *Appl. Phys. Lett.* **100** 031906
- [7] Li Y, Sinitsyn N, Smith D L, Reuter D, Wieck A D, Yakovlev D R, Bayer M and Crooker S A 2012 *Phys. Rev. Lett.* **108** 186603
- [8] Dabhashi R, Hübner J, Berski F, Pierz K and Oestreich M 2014 *Phys. Rev. Lett.* **112** 156601
- [9] Ryzhov I I, Poltavtsev S V, Kavokin K V, Glazov M M, Kozlov G G, Vladimirova M, Scalbert D, Cronenberger S, Kavokin A, V, Lemaitre A, Bloch J and Zapasskii V S 2015 *Appl. Phys. Lett.* **106** 242405
- [10] Berski F, Hübner J, Oestreich M, Ludwig A, Wieck A D and Glazov M M 2015 *Phys. Rev. Lett.* **115** 176601
- [11] Roy D, Yang L, Crooker S A and Sinitsyn N A 2015 *Scientific Reports* **5** 9573
- [12] Li F, Saxena A, Smith D and Sinitsyn N A 2013 *New J. Phys.* **15** 113038
- [13] Li F and Sinitsyn N A 2016 *Phys. Rev. Lett.* **116** 026601
- [14] Horn H, Müller G M, Rasel E M, Santos L, Hübner J and Oestreich M 2011 *Phys. Rev. A* **84** 043851
- [15] Zapasskii V S, Greilich A, Crooker S A, Li Y, Kozlov G G, Yakovlev D R, Reuter D, Wieck A D and Bayer M 2013 *Phys. Rev. Lett.* **110** 176601
- [16] The DAC is designed and made by ourselves similar to that used by Crooker *et al.* (Ref. [5])
- [17] Franz F A and Volk C 1976 *Phys. Rev. A* **14** 1711
- [18] Lucivero V G, Jiménez-Martínez R, Kong J and Mitchell M W 2016 *Phys. Rev. A* **93** 053802
- [19] Seltzer S J 2008 *Developments in Alkali-metal Atomic Magnetometry* (Ph. D. Dissertation) (Princeton: Princeton University).
- [20] He L X and Wang Y Z 2004 *Chin. Phys. B* **13** 754